Study of protective diamond-like carbon films on GCr15 bearing steel

F. Z. Yang*[1,2], L. R. Shen[1], H. L. Zhu[1], S. Q. Wang[1,2], Z. H. Wang[1,2] and H. F. Liu[1,2]

Hydrogenated diamond-like carbon (H-DLC) were deposited on GCr15 bearing steel by double cathodes pulse glow discharge (DCPGD) plasma vapour deposition at different gas volume ratios. The surface morphology, composition, microstructure, hardness and friction properties of the H-DLC films were observed. It was found that the sp^3 bond content and I(D)/I(G) ratio of DLC films were between 58 and 61% and in the range of 0·68–0·88, respectively. When $H_2 : Ar : C_2H_2$ gas volume ratio ranges from 4 : 1 : 1 to 8 : 1 : 1, the I(D)/I(G) ratio decreases with an increase in the sp^3 bond content, the friction coefficient (about 0·1) and wear rate (between $4{\cdot}5\times10^{-8}$ and $8{\cdot}4\times10^{-8}$ mm^3 N^{-1} m^{-1}) of DLC films were very low. In this study, when $H_2 : Ar : C_2H_2$ gas volume ratio is 6 : 1 : 1, the thickness of the film is 8·13 μm deposited for is 4 h, the hardness reaches a maximum value (22·5 GPa), the friction coefficient and wear rate reduce to a minimum value, 0·094 and $4{\cdot}5\times10^{-8}$ mm^3 N^{-1} m^{-1}, respectively.

Keywords: DCPGD, DLC, Composition, Microstructure

Introduction

Diamond-like carbon (DLC) films are also one of the most considerably investigated films due to their favourable properties, such as high hardness,[1,2] high wear resistance,[3] low friction coefficient,[4] chemical inertness,[5] high elastic modulus, electrical insulation property,[6] thermal conductivity, biocompatibility[7] and optical transparency in the visible and infrared.[8] Therefore, DLC films are widely used in mechanical, chemical, acoustic, electronic, optical and biomedical fields.

The major disadvantage of DLC film is that it can lead to a large stress in the film, which can make the thicker film delaminate especially for ferrous metal substrate like this. H-DLC films have attracted and still attract attention in study for their low temperature deposition and their hybrid properties ranging from DLC. There are many plasma enhanced chemical vapour deposition (PECVD) methods to study the H-DLC films, for example, microwave PECVD,[9,10] direct current glow discharge PECVD,[11] pulse glow discharge PECVD (the most pulse frequency are operated at 13·56 MHz).[12–14] These deposition methods cannot be used for industrial application owing to their low deposition rate, poor performance, and high cost. In this paper, the power supply of pulse discharge equipment is independent of two cathodes in parallel. Then, the plasma generates high energy by the different electric filed distribution of two cathodes. Raman spectroscopy is a popular, effective and non-destructive tool for structural characterisation of DLC films.[15–18] Most light sources are visible light; however, the visible light is easy to produce fluorescence effect and influence Raman spectroscopic analysis. In this work, the 325 nm ultraviolet light excitation source was selected. H-DLC films were prepared by using two mutually parallel cathodes method with H_2, C_2H_2 and Ar. All samples were characterised with optical microscopy, surface profilometer, Fourier transform infrared spectroscopy (FTIR), X-ray photoelectron spectroscopy (XPS), atomic force microscopy (AFM), Raman spectroscopy, hardness testing machine and friction and wear test machine. In this way, the thick DLC films can be prepared by double cathodes pulse glow discharge (DCPGD) plasma vapour deposition.

Experimental details

The experiment is performed on a plasma depositing equipment developed by Southwestern Institute of Physics in China by using the infiltration and injection technique, as shown in Fig. 1. The GCr15 bearing steel in specification of $40\times20\times3$ mm is used as the substrate. Before the experiment, the substrate is cleaned with alcohol and acetone in an ultrasonicator for 15 min, dried in a desiccator and then placed under vacuum. Before the deposition, the vacuum chamber is heated to 300°C and the pressure was smaller than $3{\cdot}0\times10^{-3}$ Pa. Then, 200 SCCM (standard cubic centimetre per minute) argon gas is injected into the vacuum chamber to reach the pressure of 3·3 Pa. Then, the substrate is cleaned by the glow discharge for 20 min.

[1]Southwestern Institute of Physics, Chengdu 610041, China
[2]The Engineering & Technical College of Chengdu University of Technology, Leshan 614000, China

*Corresponding author, email swiptc@163.com

Published by Maney on behalf of the Institute
Received 19 January 2014; accepted 1 July 2014
DOI 10.1179/1743294414Y.0000000327

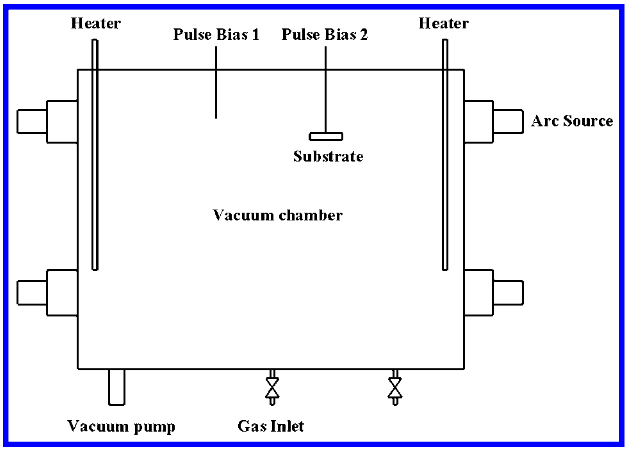

1 Schematic diagram of plasma depositing equipment

The pulse frequency and pulse duration are 30 kHz and 8 μs, respectively. Their adjustable processing parameters are listed in Table 1. The surface morphology of films were observed with a CSPM5500 AFM, which was operated in tapping mode with the scanning frequency of 1 Hz and the scanning area of over 108 × 108 nm. The chemical composition and chemical state of the films were evaluated using FTIR and XPS. The XPS with an Al K_α monochromatic excitation source of 1486·6 eV was utilised. The emitted photoelectrons were detected with a concentric hemispherical analyser at pass energy of 29·4 eV. The Raman spectra of the DLC films were tested with the Labram HR800 spectrometer produced by Jobin Yvon Company in France. The 325 nm UV laser was used as the excitation source and the spot diameter of focus measurement is 1 μm. To ensure that the signal measured is of a real feature of a-C : H samples, the samples rotating at a very high speed of 3000 rev min^{-1} were performed, and a low input power of 0·5 mW was used in order to minimise possible beam-heating effects. The chemical bonding configurations were characterised by FTIR at room temperature using BRUKER instrument to investigate the various chemical vibrational modes. The spectrum was recorded in the region of 4000–950 cm^{-1} and 60 scans were done at a resolution of 4 cm^{-1}. Hardnesses of all the DLC films were measured using a CSEM nanoindenter. Friction tests were carried out using an MS-T3000 at room temperature. This is based on a rotating ball-on-disc configuration. The friction test conditions used in this study were: applied load 4·96 N, rotation speed was 500 cycles per minute and the total sliding distance was 1256 m. For each value the tests were carried out twice. The wear scar morphology of DLC films was observed using optical microscopy, and depth and width of wear scars were measured with surface profilometer, then the formula used to calculate the volume of a wear scar is $w_V = \frac{t(3t^2+4b^2)}{6b}2\pi r$, where w_V is volume loss, t is depth of wear scar, b is width of wear scar, and r is the radius of the wear scar.

Results and discussion

Surface morphology

Figure 2 shows the representative AFM topography images of the DLC films obtained on the GCr15 substrate at different $H_2 : Ar : C_2H_2$ gas volume ratios. The AFM demonstrates the formation of uniform and smooth films. The surface roughness of DLC films was between 0·4 and 0·9 nm.

XPS data

Figure 3*a*–*c* indicates the deconvolution of XPS spectra of the DLC films deposited at different gas volume ratios. The raw spectra obtained begin with the removal of the ubiquitous background present in the core spectra. The Shirley background subtraction procedure was performed to analyse the XPS data. The sp^3 content [$\eta(sp^3)$] in DLC films was evaluated by XPS fitting for C1s core peak, consisting of bands due to diamond (285·2 eV) and graphite (284·4 eV) phases. Since the area of each peak was directly related to the concentration of the corresponding phase, the sp^3 content was deduced from the ratio of diamond peak area (S_1) over the sum of diamond peak area and graphite peak area

Table 1 Major parameters of DLC films generated by using DPGD method (316LN)

Gas pressure/Pa	Gas flowrate $H_2 : Ar : C_2H_2$ (SCCM)	Pulsed voltage 1 and 2/V	Thickness/μm	Time/min
12	4 : 1 : 1 (120 : 30 : 30)	1000/4500	7·90	240
12	6 : 1 : 1 (180 : 30 : 30)	1000/4500	8·13	240
12	8 : 1 : 1 (240 : 30 : 30)	1000/4500	8·08	240

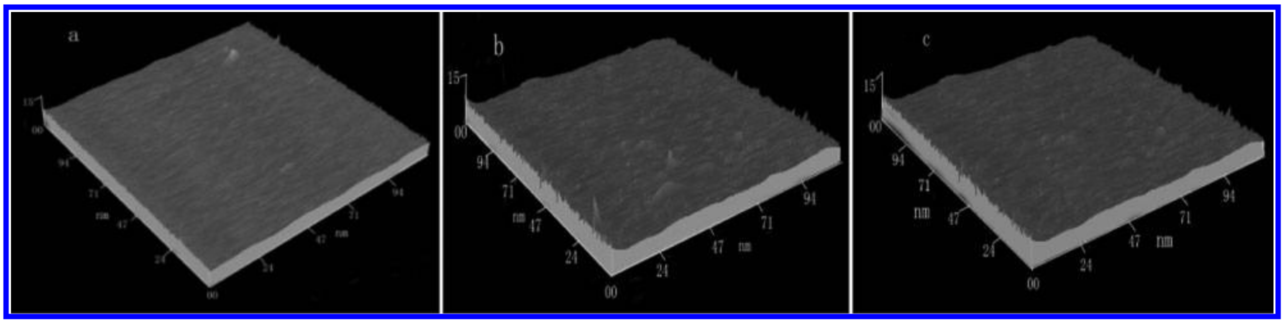

2 Typical AFM image of different gas volume ratios: *a* 4 : 1 : 1; *b* 6 : 1 : 1; *c* 8 : 1 : 1

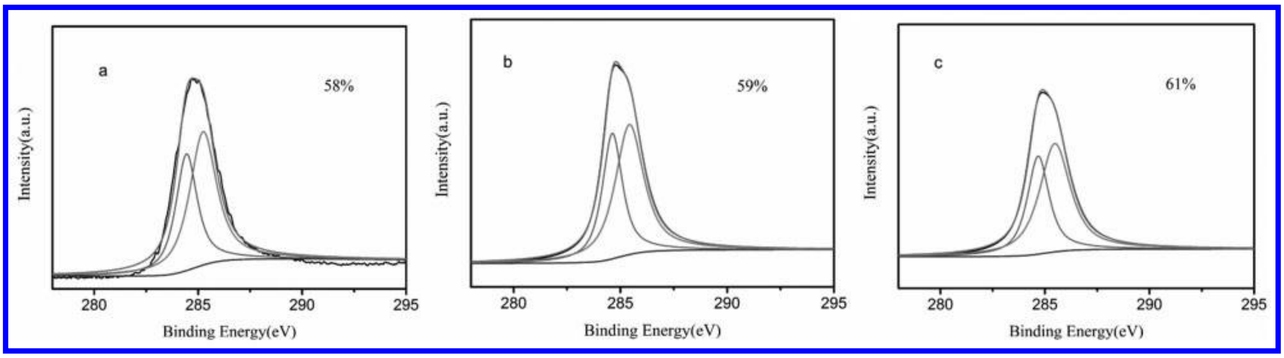

3 Deconvolution of XPS C1s peaks of DLC films: *a* 4 : 1 : 1; *b* 6 : 1 : 1; *c* 8 : 1 : 1

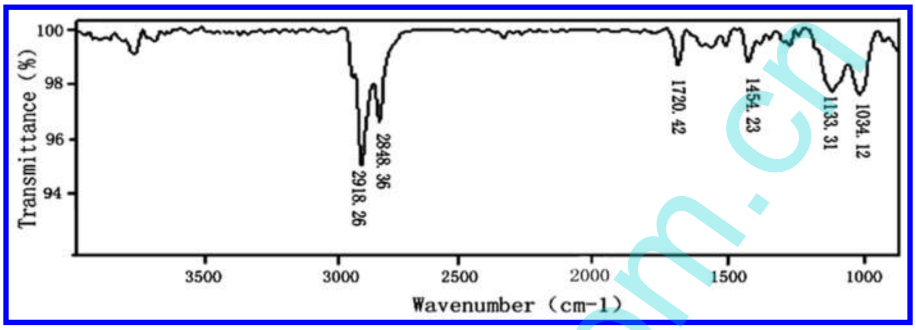

4 Spectrum (FTIR) of DLC film prepared by with various gas volume ratios

(S_2), η (sp^3)=$S_1/(S_1+S_2)$. The XPS spectrum was profile fitted by a Gaussian and Lorentzian method, and the contribution of the background was approximated by the Shirley method. As a result, the presumable sp^3 content of the samples increases from 58 to 61%, when H_2 : Ar : C_2H_2 gas volume ratio ranges from 4 : 1 : 1 to 8 : 1 : 1, and it estimates the full widths at half maximum (FWHMs) (SP^2) and FWHMs (SP^3) of the DLC films are 1·3, 1·2, 1·1 eV, and 1·8, 1·9 and 2·0 eV respectively. In a-C : H, a higher sp^3 content is achieved mainly by H saturating C=C bonds as CH_x groups, rather than by increasing the fraction of C–C sp^3 bonds. In order to verify the fact, we evaluated the DLC film when H_2 : Ar : C_2H_2 gas volume ratio is 4 : 1 : 1 by FTIR, as shown in Fig. 4. The FTIR absorption consists of C–H stretching modes at 2800–3200 cm^{-1} and C–C modes and C–H bending modes below 2000 cm^{-1}. The peak intensity at 2800–3200 cm^{-1} is large. The FTIR curves show that the peak at around 2920 cm^{-1} is of anti-symmetric stretching vibrations of sp^3 bonded CH_2 group, and the peak at 2850 cm^{-1} is of symmetric stretching vibrations of sp^3 bonded CH_2 group or CH_3 group. The peaks are consistent with the results obtained by Khettache *et al.*[19] At the same time, the peaks around 1450, 1136 and 1032 cm^{-1} also are sp^3 – C–$H_{(2,3)}$ modes.

Raman analysis

Figure 5 shows the UV Raman spectra at different gas volume ratios by fitting the peak. Raman spectra of DLC films had a typical DLC broad peak (G-band)) and a shouldered peak (D-band) by Gaussian curve fitting. Generally, the Raman spectra of the diamond have a sharp characteristic peak around 1332 cm^{-1} region, caused by the vibrations of sp^3 atom. The Raman spectra of the single crystal graphite have a characteristic peak around 1560 cm^{-1}, which is called G peak. The Raman spectra of the disordered graphite have a characteristic peak around 1360 cm^{-1}, which is called D peak. As shown in the following figures, when gas volume ratios are different, the G peak and D peak positions are different and the I(D)/I(G) ratio of the DLC films from 0·68 to 0·88.

Hardness

Figure 6 shows the hardness of DLC films at different gas volume ratios. When H_2 : Ar : C_2H_2 gas volume ratio is 6 : 1 : 1, the DLC films do display high hardness value 22·5 GPa; when H_2 : Ar : C_2H_2 gas volume ratio is 8 : 1 : 1, the hardness is 19·9 GPa, which is lower than the H_2 : Ar : C_2H_2 gas volume ratio is 6 : 1 : 1. The reason is that the films are composed of carbon–hydrogen bonds, When sp^3 content is greater than 60%, the hardness value will decrease. The conclusions are consistent with those proposed by Ferrari and Robertson[20]

Friction and wear

Figure 7 shows the friction coefficient of GCr15 substrate and DLC films at different gas volume rates. The friction and wear properties of the DLC films were investigated and the results show that they have a very

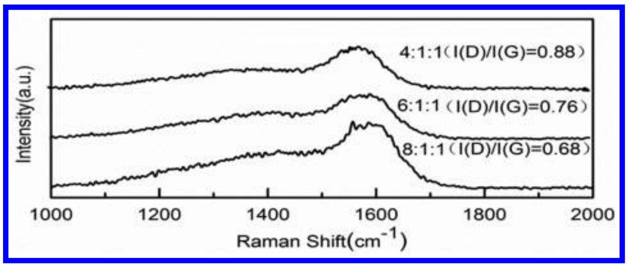

5 DLC films Raman spectra

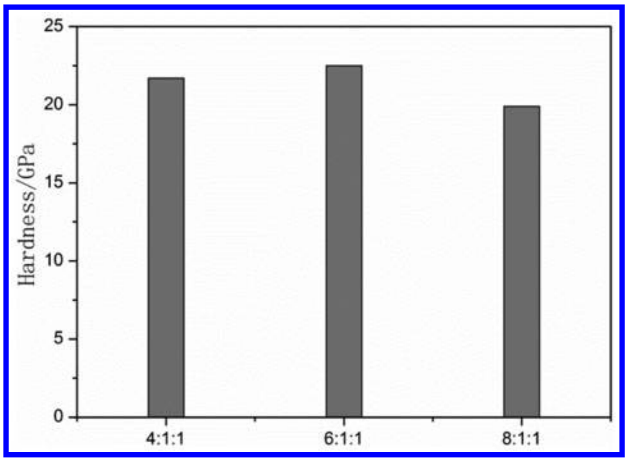

6 Influence of $H_2:C_2H_2:Ar$ gas volume ratios on hardness

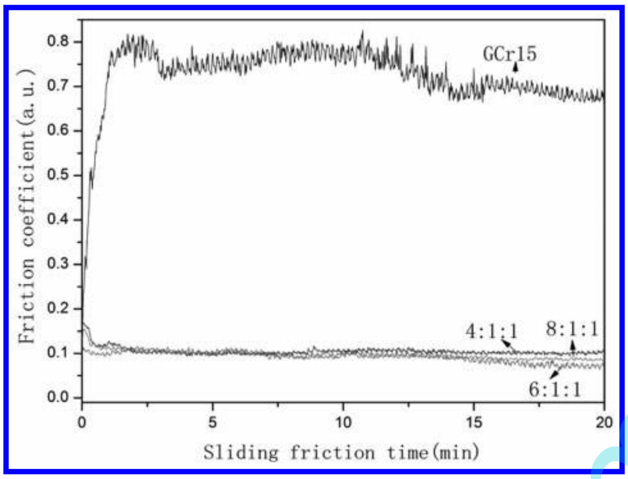

7 Friction coefficient of GCr15 and different $H_2:C_2H_2:Ar$ gas volume ratios

low coefficient of friction of about 0·1. When $H_2:Ar:C_2H_2$ gas volume ratio is 6 : 1 : 1, the coefficient of friction is 0·094 and it is minimum value. However, the friction coefficient of the GCr15 substrate is very large, about 0·725. It can be found that the friction and wear performance improvement are very significant.

The wear rates of DLC films are shown in Fig. 8. In air environment, the wear rate of every DLC film was clearly lower than GCr15 substrate and it was a very low value in the about $4{\cdot}5\times10^{-8}$–$8{\cdot}4\times10^{-8}$ mm^3 N^{-1} m^{-1} ranges. The wear rate tends to decrease with increasing film hardness.

Friction surface

Figure 9 shows friction surface features of DLC films and GCr15 substrate. Wear debris is visible around the friction surface of GCr15 substrate and transferred material is relatively little. The average width of the scratch is 603 μm of GCr15 substrate and the average width of the scratch in DLC films varied from 245 to 263 μm. The wear of DLC films hardly occurred. Figure 9 shows the optical images of the wear track of the GCr15 substrate along with a stable wear profile of DLC films.

The main factors affecting the friction and wear between the two objects are the adhesion between the microscopic asperities in the contact region as reported by Bowden and Tabo.[21,22] The coefficient of friction (μ) of the film is calculated as follows

$$\mu=\frac{F}{W}=\frac{\tau A}{W}=\frac{\tau}{p}$$

where, F, W, p, τ and A is the tangential force, normal force, point of contact pressure, shear strength and contact area respectively. According to this formula, if the two hard surfaces are in contact with each other, the contact area is small, but the shear strength is larger. Therefore it will lead to increasing friction coefficient. Similarly, if one or both of the softer surface contact, the shear strength is small, but the contact area is large, it will also lead to increasing of friction coefficient. However, if there is an isolation relatively soft layer in contact between two hard surfaces, the contact area and the shear strength all are

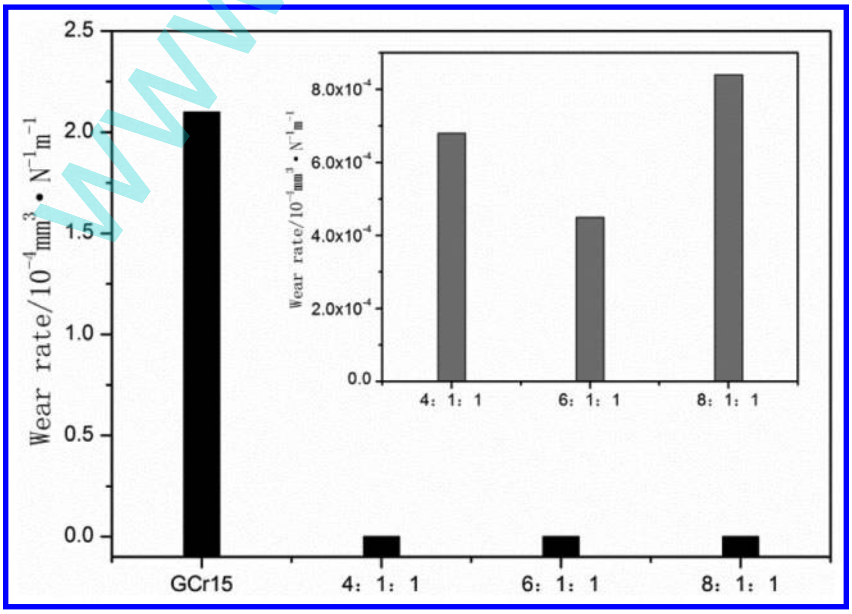

8 Wear rate of GCr15 and different $H_2:C_2H_2:Ar$ gas volume ratios

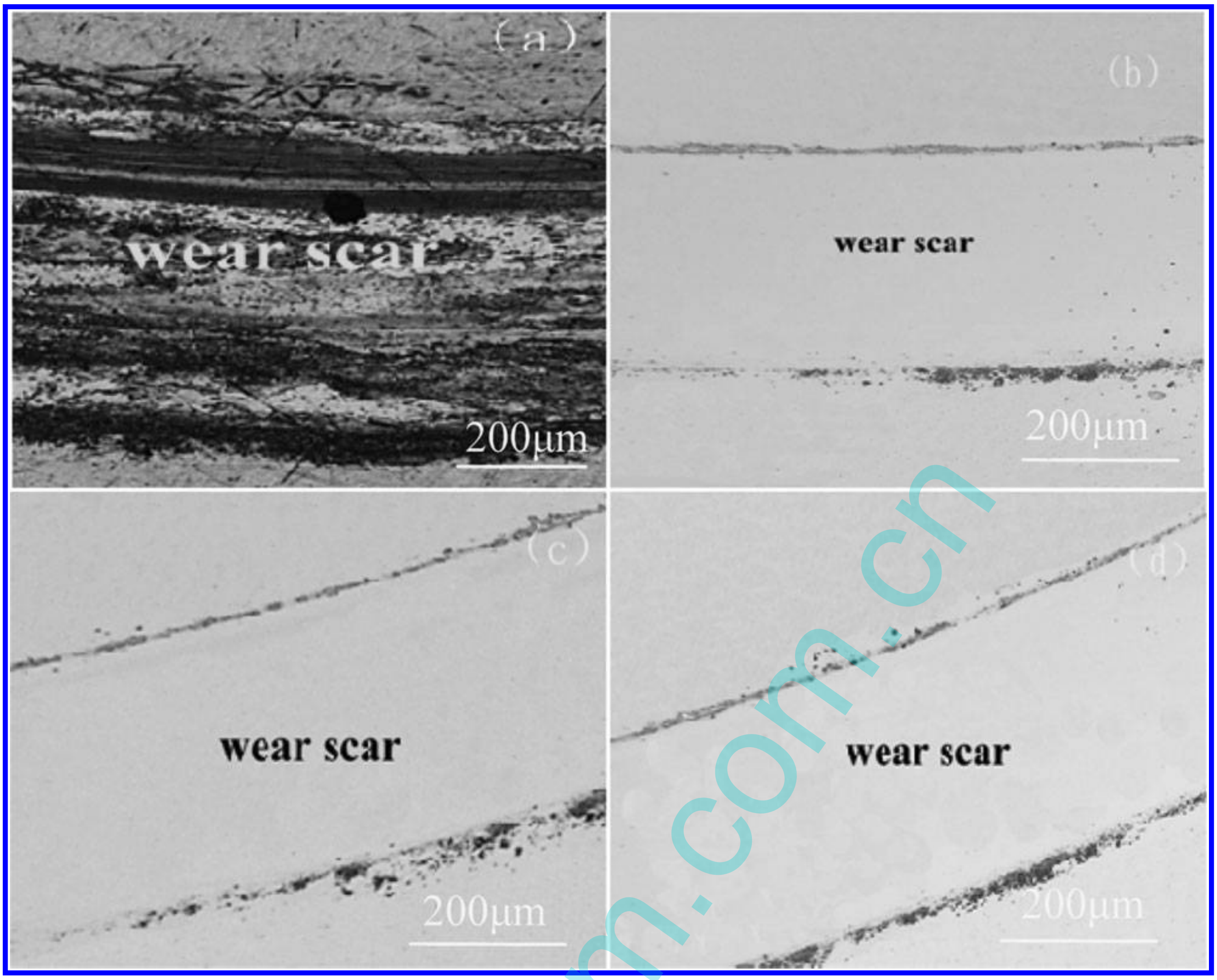

9 Friction surface features: *a* GCr15 substrate; *b* 4 : 1 : 1; *c* 6 : 1 : 1; *d* 8 : 1 : 1

small. Generally, DLC films are developed for anti-friction layer and wear layer by the principle.

Conclusion

1. The DLC films were deposited at 300°C using the DCPGD plasma vapour deposition at different gas flowrates.

2. It is found that when $H_2:Ar:C_2H_2$ gas volume ratio is from 4 : 1 : 1 to 8 : 1 : 1, the sp^3 content of the samples increases from 58 to 61%. The I(D)/I(G) ratio of DLC films was between 0·88 and 0·68.

3. When $H_2:Ar:C_2H_2$ gas volume ratio is from 4 : 1 : 1 to 8 : 1 : 1, the wear rate of every DLC film was clearly lower than GCr15 substrate and it was a very low value in the about $4\cdot5\times10^{-8}$–$8\cdot4\times10^{-8}$ mm^3 N^{-1} m^{-1} ranges.

4. DLC film showed high sp^3 bond content, when $H_2:Ar:C_2H_2$ gas volume ratio is 8 : 1 : 1, and the maximum hardness (22·5 GPa) and FWHM (G) value, the minimum friction coefficient value (0·094) and wear rate ($4\cdot5\times10^{-8}$ mm^3 N^{-1} m^{-1}) appeared at $H_2:Ar:C_2H_2$ gas volume ratio is 6 : 1 : 1.

5. The friction coefficient and wear rate tend to decrease with increasing film hardness.

Acknowledgment

This work was supported by the National Natural Science Foundation of China (grant no. 11205050).

References

1. Y. S. Zou, Y. F. Wu, H. Yang, K. Cang, G. H. Song, Z. X. Li and K. Zhou: *Appl. Surf. Sci.*, 2011, **258**, (4), 1624–1629.
2. G. Cicala: *Surf. Eng.*, 2012, **28**, 141–144.
3. B. Vengudusamy, J. H. Green, G. D. Lamb and H. A. Spikes: *Wear*, 2013, **298–299**, 109–119.
4. Z. Y. Hu, A. Schubnov and F. Vollertsen: *J. Mater. Process. Technol.*, 2012, **3**, 647.
5. Y. Yamauchi, Y. Sasai, S. Kondo and M. Kuzuya: *Thin Solid Films*, 2010, **518**, 3492–3496.
6. V. M. Tiainen, A. Soininen, E. Alakoski and T. Yrjö Konttinen: *Diamond Relat. Mater.*, 2008, **17**, 2071–2074.
7. M. S. Amin, L. K. Randeniya, A. Bendavid, P. J. Martin and E. W. Preston: *Diamond Relat. Mater.*, 2012, **21**, 42–49.
8. O. M. Kutsay, A. G. Gontar and N. V. Novikov: *Diamond Relat. Mater.*, 2001, **10**, 1846–1849.
9. R. Matsui, K. Mori, H. Kousaka and N. Umehara: *Diamond Relat. Mater.*, 2013, **31**, 72–80.
10. S. Kumar, C. M. S. Rauthan, P. N. Dixit, K. M. K. Srivatsa, M. Y. Khan and R. Bhattacharyya: *Vacuum*, 2001, **63**, 433–439.
11. J. S. Hsu, S. S. Tzeng and Y. J. Wu: *Vacuum*, 2009, **83**, 622–624.
12. X. L. Shi, Q. L. Wang, L. L. Xu, S. Ge and C. Wang: *Appl. Surf. Sci.*, 2009, **255**, 8246–8251.

13. S. F. Ahmed, M. K. Mitra and K. K. Chattopadhyay: *Appl. Surf. Sci.*, 2007, **253**, 5480–5484.
14. G. Fedosenko, A. Schwabedissen, J. Engemann, E. Braca, L. Valentini and J. M. Kenny: *Diamond Relat. Mater.*, 2002, **11**, 1047–1052.
15. Y. Y. He, G. F. Zhang and V. Buck: *Diamond Relat. Mater.*, 2011, **20**, 97–100.
16. S. Urbonaite, L. Hälldahl and G. Svensson: *Carbon*, 2008, **46**, (14), 1942–1947.
17. M. Ali, M. Ürgen and A. Kawashima: *Surf. Eng.*, 2012, **28**, 791–795.
18. M. Foong, A. T. T. Koh, S. R. Lim, J. Hsieh and D. H. C. Chua: *Diamond Relat. Mater.*, 2012, **25**, 103–110.
19. A. Khettache, T. Staedler, M. Z. Touhami, H. Weiß and X. Jiang: *Surf. Eng.*, 2013, **29**, 474–478.
20. A. C. Ferrari and J. Robertson: *Phys. Rev. B*, 2001, **64B**, 1–13.
21. F. P. Bowden and D. Tabor: 'The friction and lubrication of solids', Part I, 230; 1950, Oxford, Clarendon Press.
22. F. P. Bowden and D. Tabor: 'The friction and lubrication of solids', Part II, 10; 1964, Oxford, Clarendon Press.